European Journal of Medicinal Chemistry 44 (2009) 3504–3508

Contents lists available at ScienceDirect

European Journal of Medicinal Chemistry

journal homepage: http://www.elsevier.com/locate/ejmech

Original article

Potential of mean force for Syrian hamster prion epitope protein – Monoclonal fab 3f4 antibody interaction studies

Yeng-Tseng Wang [a,b], Zhi-Yuan Su [c], Jun-Min Liao [b], Cheng-Lung Chen [b,*]

[a] National Center for High-performance Computing, Hsin-Shi, Tainan County, Taiwan, ROC
[b] The Department of Chemistry, National Sun Yat-Sen University, Kaohsiung 804, Taiwan, ROC
[c] The Department of Information Management, Chia Nan University of Pharmacy and Science, Tainan 717, Taiwan, ROC

ARTICLE INFO

Article history:
Received 4 July 2008
Received in revised form
27 August 2008
Accepted 17 December 2008
Available online 31 December 2008

Keywords:
Molecular dynamics
Potential of mean force
Prion
Antibody

ABSTRACT

Simulating antigen–antibody interactions are crucial for understanding antigen–antibody associations in immunology. To shed further light on this question, we study a dissociation of the Syrian hamster prion epitope protein–fab 3f4 antibody complex structure. The stretching, that is, the distance between the center of mass of the prion epitope protein and the fab 3f4 antibody, has been studied using potential of mean force (PMF) calculations based on molecular dynamics (MD) and the implicit water model. For the complex structure, there are four important intermediates, U-shaped groove on the antibodies, and two inter-protein molecular hydrogen bonds in the stretching process. Use of our simulations may help in understanding the binding mechanics of the complex structure, and thus of significance in the design of antibodies against prion disease.

1. Introduction

Stretching mechanics is an important factor for understanding antigen–antibody associations and improving antigen–antibody binding efficiency in immunology. The cellular prion protein (PrP^C) is an essential element in the pathogenesis of a group of human and animal neurodegenerative diseases, which include bovine spongiform encephalopathy in cattle, scrapie in sheep, Creutz-feldt–Jacob disease, Gerstmann–Staussler syndrome and fatal familiar insomnia in humans [1,2]. The accumulation of the scrapie isoform (PrP^{Sc}) of the prion protein leads to these prion association diseases. The formation of the PrP^{Sc} from the PrP^C is a post-translational process without candidate chemical modifications, and the conversion involves substantial changes in the secondary structure of the protein with PrP^C containing α-helices and with PrP^{Sc} enriched in β-sheets [3]. From an X-ray experiment, Cohen et al. [4] shows the U-shaped groove on the antibodies (Tyr32, Ile34, Tyr252, Trp89, Gly91, His95, Trp269, Asp271, Glu272, Asn276, and Gln278) and two intermolecular hydrogen bonds may play important roles in binding the specific epitope of PrP^{Sc} [5]. However, the protein–protein binding mechanics is difficult to track by experimental methods, and thus MD simulations have been more readily applied to analyze the complex structure binding mechanics.

The PMF method is a practical application to better understand the binding interactions between two group molecules. For biological systems like the binding force of the double helix DNA [6] and the lysozyme–antibody interactions [7], the PMF is calculated for analyzing the intermolecular interactions. Our PMF calculations of stretching the complex structure from equilibrium MD simulations were performed with umbrella sampling techniques and the weighted histogram analysis method (WHAM). Computations on the stretching of the complex structure were performed in a generalized Born (GB) solvent model [8] instead of an explicit solvent model [9]. The GB [10–16] solvent model is suitable to protein macromolecules and more efficiently used to account for the solvent effect. The stretching distance is from 3.0 nm to 6.0 nm.

In the present study, MD simulations were performed to study the stretching of the prion–antibody complex structure. Detailed analysis of the MD simulations revealed the PMF, the profile of cumulate changed dihedral angles (CCDAs), the pair interactions of the U-shaped groove-prion epitope, the root mean square displacement (RMSD) of the U-shaped groove, and the distance trajectories of the two hydrogen bon ds (DTOHB) in the stretching process.

* Corresponding authors. The Department of Chemistry, National Sun Yat-Sen University, Kaohsiung 804, Taiwan, ROC. Tel.: +886 7 5252630; fax: +886 5050940.
E-mail address: chen@mail.nsysu.edu.tw (C.-L. Chen).

0223-5234/$ – see front matter © 2009 Elsevier Masson SAS. All rights reserved.
doi:10.1016/j.ejmech.2008.12.023

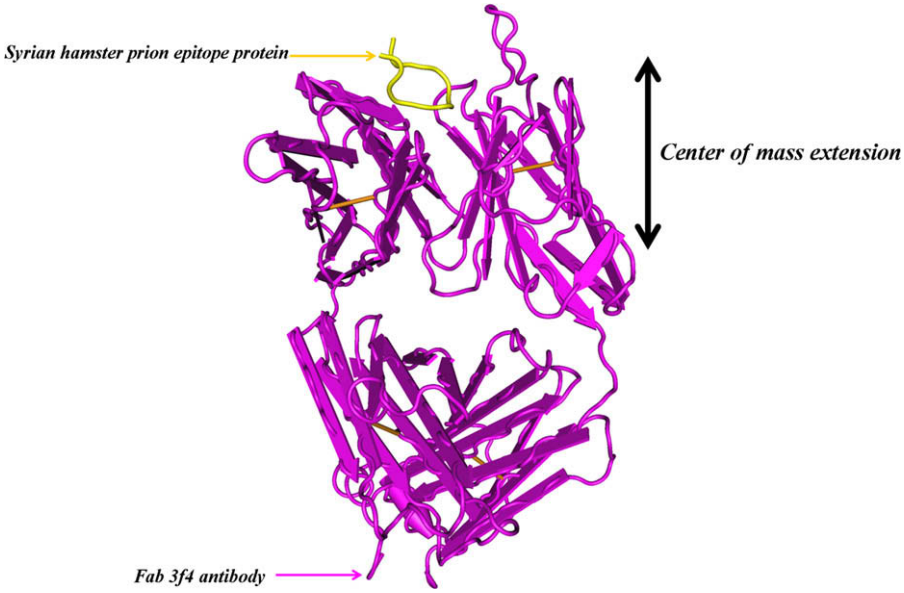

Fig. 1. Model for the stretching (center of mass extension) simulation on the Syrian hamster prion epitope protein–fab 3f4 antibody complex.

2. Methods

2.1. Initial model systems of the prion epitope protein–antibody complex

Several prion–antibody complex structures were dissolved and deposited in protein data banks [4,17]. We used the X-ray structure of the Syrian hamster prion epitope protein–fab 3f4 antibody complex (PDB ID: 1CU4) as the initial model because the interactions of the complex structures have been well studied by Cohen et al. [4]. This model was assigned protonation states at pH 7.0 [18], and is shown in Fig. 1.

2.2. Computational models and details

Calculations were performed with the software program Charmm [19] using the Charmm parameters (par_all27_prot_na) and the GB solvent model. All MD simulations were performed in the canonical ensemble [20] (the simulation temperature is equal to 310 K), unless noted, using the Verlet integrator, an integration time step of 0.002 ps and SHAKE [21] of all covalent bonds involving hydrogen atoms. Atoms based truncation was conducted using shift electrostatic and switch van der Waals functions with a 1.8 nm cutoff for atom-pair lists. The complex structure was minimized for 10,000 conjugate gradient steps, and this minimized complex structure was then subjected to a 1 ns isothermal, constant volume MD simulation. The final structure was used to initiate the PMF calculations and the MD trajectories were used to obtain the normal CCDAs' calculations.

2.3. Potential of mean force calculations (Helmholtz free energy)

The Charmm miscellaneous mean field potential (MMFP) was applied in the stretching constraints. The PMF calculations used a reaction coordinate (r), defined as the distance between the center of mass of the prion epitope protein and the fab 3f4 antibody, to describe the complex structure binding mechanics. The r value was varied from 3.0 nm to 6.0 nm in 0.1 nm increments. The MD simulations for PMF determination were performed with an initial 0.5 ns equilibration followed by 1 ns of sampling at a given r.

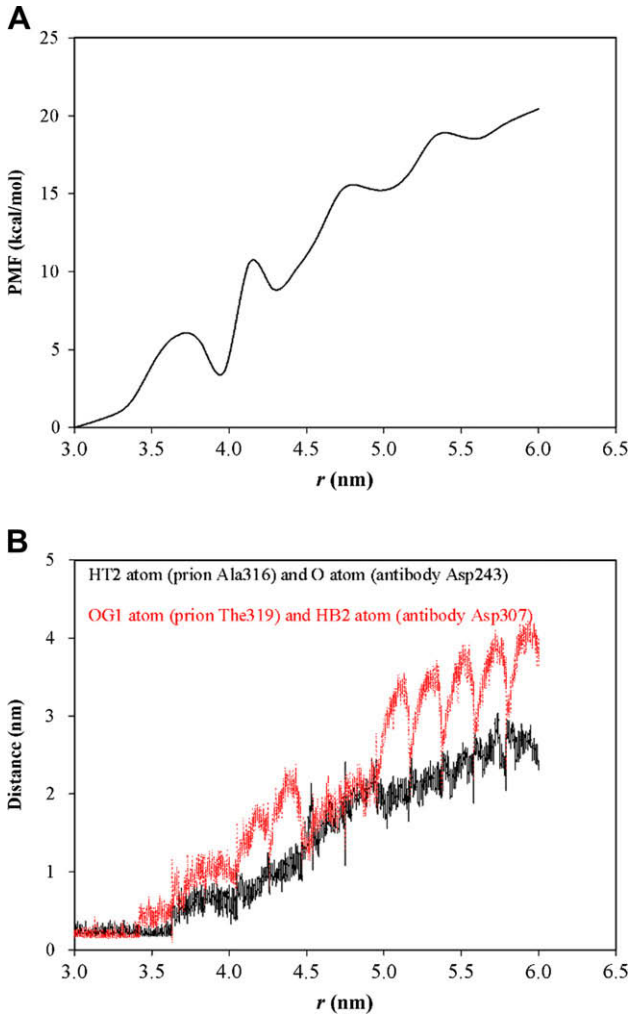

Fig. 2. (A) The calculated PMF profile (r of 3.0–6.0 nm). (B) The distance trajectories of the two intermolecular hydrogen bonds.

Table 1
The normal range of amino residues' CCDAs (the Syrian hamster prion epitope protein–fab 3f4 antibody complex structure).

Amino residue	Cumulative changes in dihedral angles/degree			
	Maximum of phi (Φ)	Maximum of psi (Ψ)	Average of phi (Φ)	Average of psi (Ψ)
ALA	92.00	136.00	14.00	16.00
ARG	106.00	90.00	22.00	16.00
ASN	93.00	224.00	14.00	19.00
ASP	100.00	159.00	13.00	23.00
CYS	84.00	143.00	13.00	23.00
GLN	97.00	186.00	17.00	14.00
GLU	108.00	100.00	19.00	15.00
GLY	231.00	297.00	20.00	20.00
HSD	96.00	86.00	14.00	14.00
ILE	73.00	47.00	11.00	9.00
LEU	114.00	62.00	16.00	12.00
LYS	292.00	69.00	16.00	11.00
MET	52.00	97.00	13.00	14.00
PHE	73.00	55.00	14.00	11.00
PRO	67.00	122.00	16.00	15.00
SER	117.00	93.00	18.00	15.00
TRP	83.00	63.00	13.00	13.00
TYR	77.00	112.00	12.00	13.00
VAL	74.00	78.00	13.00	11.00

The WHAM [22] method was used to analyze molecular dynamics or monte carlo simulation data. WHAM minimizes the error in the density-of-states function and facilitates the calculations of free energy surfaces. In each simulation, two quantities were monitored: the total system potential energy (V) and the total numbers of r (N_{NL}). Calculating the density-of-states function (Ω) for two quantities is computationally impractical. Thus it was necessary to calculate several Ω, each a function of different thermodynamic parameters. The formula of Ω is

$$\Omega\ (V,\ N_{NL}) = \frac{\sum_{j=1}^{k} N_k(V,\ N_{NL})}{\sum_{j=1}^{k} n_j\ \exp\left(-f_j - \beta_j V\right)} \tag{1}$$

where N_{NL} and V are the monitored parameters, N_k is the number of occurrences for sampling with (V, N_{NL}), f_j is equal to βA_j where A_j is the free energy of simulation j, β are $1/k_BT$, k is the number of simulations, and n_j is the number of samples form simulation j. The free energies were calculated by solving

$$P_\beta(V,\ N_{NL}) = \frac{\sum_{i=1}^{k} N_i(V,\ N_{NL})\ \exp(-\beta V)}{\sum_{j=1}^{k} n_j\ \exp\left(-f_j - \beta_j V\right)} \tag{2}$$

$$\exp(-f_k) = \sum_{V,\ N_{NL}} P_{\beta_k}(V,\ N_{NL}) \tag{3}$$

where P_β is the probability of observing a sample with (V, N_{NL}). Thermodynamic averages are calculated from

$$< N_{NL} > = \frac{\sum_{V,\ N_{NL}} (N_{NL})^* \Omega(V,\ N_{NL})\ \exp(-\beta V)}{\sum_{V,\ N_{NL}} \Omega(V,\ N_{NL})\ \exp(-\beta V)} \tag{4}$$

using N_{NL} as an example. Free energies are calculated via

$$F(N_{NL}) = -k_B T\ \ln\left\{P_\beta(N_{NL})\right\} \tag{5}$$

$$P_\beta(N_{NL}) = \sum_V P_\beta(V,\ N_{NL}) \tag{6}$$

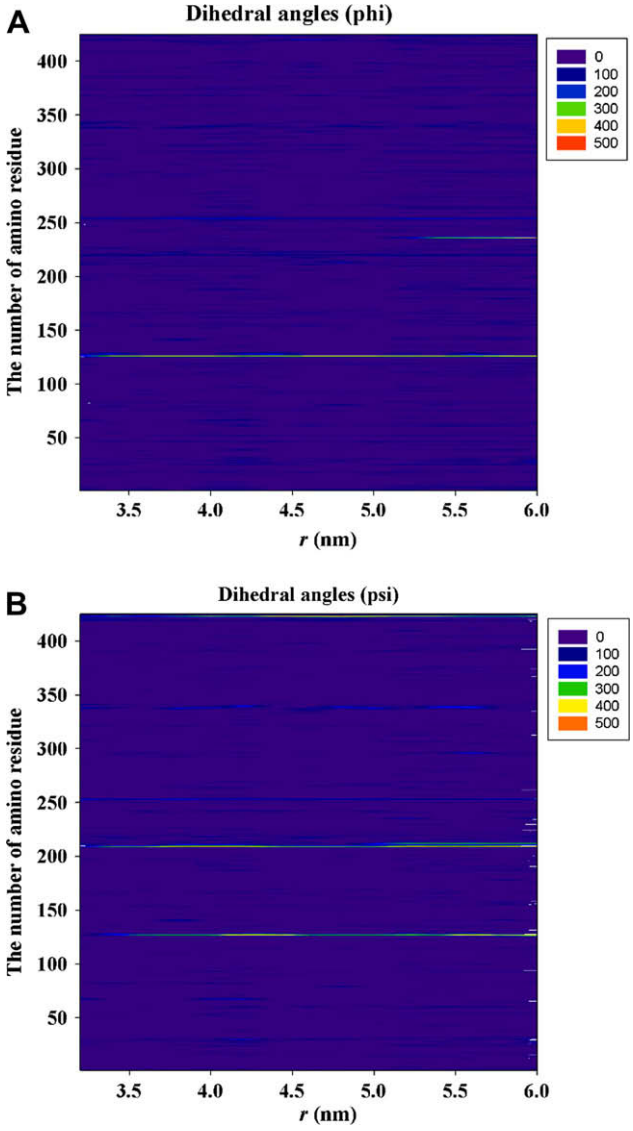

Fig. 3. A profile of cumulate changed dihedral angles (phi and psi) for the value of r from 3.0 nm through 6.0 nm. Here the amount of amino residues: 1–315 and 326–425 (antibody), 316–325 (Syrian hamster prion epitope protein).

All our PMF calculations were based on the Allen's WHAM program [23].

3. Results and discussion

3.1. PMF profile, DTOHB, and normal range of CCDAs

The PMF profile is shown in Fig. 2A and there were four major energy barriers (r was equal to 3.74, 4.15, 4.79, and 5.39 nm) in the stretching process. The distance trajectories of the two intermolecular hydrogen bonds are shown in Fig. 2B and the two bonds occurred in the r of 3.00–3.70 nm.

The normal range of CCDAs is shown in Table 1. The average of the all amino CCDAs was less than 30 degrees and the maximum of CCDAs was less than 300 degrees. From the results it seems that the large CCDAs (more than 300 degrees) are important events in the complex binding mechanics. The stretching CCDAs are shown in Fig. 3 and the amino residues (Thr126, Ser127, Phe209, Ala236 and Val423) have obvious variations in the phi or psi angles.

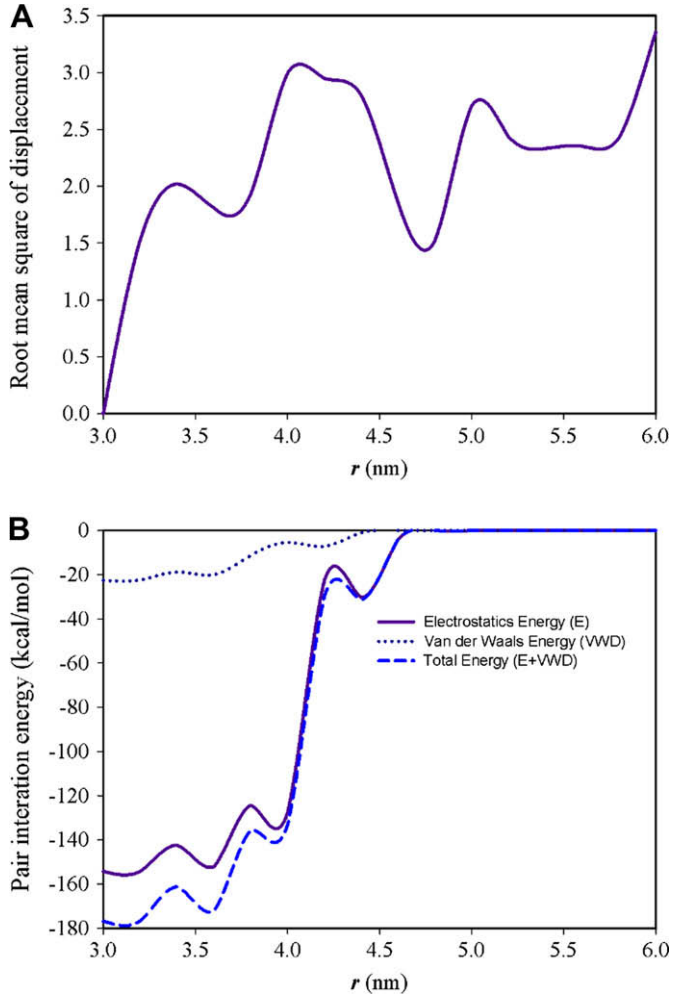

Fig. 4. (A) RMSD of U-shaped groove. (B) Pair interaction of U-shaped groove.

3.2. The RMSD and pair interactions of the U-shaped groove on the antibodies

The RMSD of the U-shaped groove is shown in Fig. 4A, and the value was less than 3.5 within the stretching process. The pair interactions of the U-shaped groove-prion epitope are shown in Fig. 4B. When the reaction coordinate r was less than 4.02 nm, the pair interactions were strong, especially for the r of 3.11 nm (equal to 150.16 kcal/mol). The pair interactions were quickly decayed within the r of 4.03–4.60 nm, and when the r was greater than 4.60 nm, the pair interactions were equal to zero.

3.3. Analysis of the four major energy barriers

The stretching CCDAs were individually traced in the four major energy barriers and the results are shown in Table 2. In the first energy barrier, the three residues (Thr126, Ser127, and Phe209) and the two hydrogen bonds (DTOHB were more than 0.5 nm) were all significant and overcame the energy barrier. The RMSD and the pair interactions (the U-shaped groove) were individually equal to 1.7 and −136.52 kcal/mol, respectively, and the energy barrier height was equal to 6.04 kcal/mol. In the second energy barrier, the three residues (Thr126, Ser127, and Phe209) had strongly rotated psi angles. The RMSD and the pair interactions (the U-shaped groove) were individually equal to 1.8 and −67.82 kcal/mol, respectively, and the energy barrier height was equal to 6.70 kcal/mol. In the third energy barrier, the two residues (Phe209 and Val423) had psi angles that were rotated more than 400.00 degrees. The RMSD and the pair interactions (the U-shaped groove) were individually equal to 1.9 and 0.00 kcal/mol, respectively, and the energy barrier height was equal to 6.50 kcal/mol. In the last energy barrier, there was only one residue (Ala236) which rotated approximately 400.00 degrees in the phi angle. The RMSD and the pair interactions (the U-shaped groove) were individually equal to 2.3 and 0.00 kcal/mol, respectively, and the energy barrier height was equal to 3.53 kcal/mol.

Table 2
The amino residues which CCDAs are more than 300 degree in the range of 3.0–3.7, 3.9–4.1, 4.3–4.7 and 5.0–5.4 nm (r).

r (nm)	The no. of amino residue	Cumulative changes in dihedral angles/degree	
		Phi (Φ)	Psi (Ψ)
3.0–3.7	Ser127	142.00	337.00
	Thr126	366.00	13.00
	Phe209	10.00	516.00
3.9–4.1	Ser127	12.00	312.00
	Thr126	12.00	345.00
	Phe209	43.00	356.00
4.3–4.7	Phe209	13.00	412.00
	Val423	26.00	457.00
5.0–5.4	Ala236	395.00	25.00

The no. of amino residue: 1–315 and 326–425 (antibody), 316–325 (Syrian hamster prion epitope protein).

Our simulation results suggest that there are four major energy barriers in the complex structure binding mechanics, and that the U-shaped groove and the five residues (Thr126, Ser127, Phe209, Ala236 and Val423) play important roles in relaxing the complex structure and making it easy to bind together. After the complex structure system overcomes the 4–2 energy barriers, the U-shaped groove and the two hydrogen bonds might help the complex structure overcome the first energy barriers more easily.

4. Conclusions

In this paper, we proposed using stretching of the prion–antibody complex structure to predict the binding mechanics and the free energy profile, and carried out the stretching prion–antibody complex MD simulations. We used the WHAM method to extract the PMF profile from the MD simulations and found four major energy barriers in the stretching process. In this work, we used cumulative changed dihedral angles (CCDAs), RMSD/pair interactions of the U-shaped groove and the two intermolecular hydrogen bonds to analyze the energy barriers. From the results obtained, we suggest that the five residues (Thr126, Ser127, Phe209, Ala236 and Val423), the U-shaped groove and the two inter-protein molecular hydrogen bonds might play important roles in the development of bioactive antibody analogues.

Acknowledgments

This work was supported by the National Center for High-performance Computing and the National Sun Yat-Sen University, Taiwan.

References

[1] M. Kaneko, N. Sugiyama, D. Sasayama, K. Yamaoka, T. Muyakawa, K. Arima, K. Tsuchiya, K. Hasegawa, S. Washizuka, T. Hanihara, N. Amano, S. Yaishita, Psychiatry. Clin. Neurosci. 62 (2008) 264–270.
[2] J.D. Wadsorth, C. Powell, J.A. Beck, S. Joiner, J.M. Lineham, S. Brandners, S. Mead, J. Collinge, Methods Mol. Biol. 459 (2008) 197–227.
[3] A. Aguzzi, C. Sigurdson, M. Heikenwalder, Annu. Rev. Pathol. 3 (2008) 11–40.
[4] Z.F. Kanyo, K.M. Pan, R.A. Williamson, D.R. Burton, S.B. Prusiner, R.J. Fletterick, F.E. Cohen, J. Mol. Biol. 293 (1999) 855–863.

[5] F.F. Yuan, S. Biffin, M.W. Brazier, M. Suarez, R. Cappai, A.F. Hill, S.J. Collins, J.S. Sullivan, D. Middleton, G. Multhaup, A.F. Geczy, C.L. Masters, Immunol. Cell Biol. 83 (2005) 632–637.
[6] A.D. Mackerell, G.U. Lee, Eur. Biophys. J. 28 (1999) 415–426.
[7] Y.T. Wang, J.M. Liao, C.L. Chen, Z.Y. Su, C.H. Chen, J.J. Hu, Chem. Phys. Lett. 455 (2008) 284–288.
[8] F.S. Lee, A. Warshel, J. Chem. Phys. 90 (1992) 3100–3107.
[9] H.J.C. Berendsen, J.R. Grigera, T.P. Straatsma, J. Phys. Chem. 91 (1987) 6269–6271.
[10] D. Bashford, D.A. Case, Rev. Phys. Chem. 51 (2000) 129–152.
[11] B. Honig, K. Sharp, A.S. Yang, J. Phys. Chem. 97 (1933) 1101–1109.
[12] P. Beroza, D.A. Case, Methods Enzymol. 295 (1998) 170–189.
[13] C.J. Cramer, D.G. Truhlar, Chem. Rev. 99 (1999) 2161–2200.
[14] J. Srinivasan, T.E. Cheatham, P.A. Kollman, D.A. Case, J. Am. Chem. Soc. 120 (1998) 9401–9409.
[15] D. Bashford, Curr. Opin. Struct. Biol. 1 (1991) 175–184.
[16] I. Massova, P.A. Kollman, J. Am. Chem. Soc. 121 (1999) 8133–8143.
[17] F. Primary, J. Grosclade, S. Lesceu, B. Doublet, E. Treguer, H. Rezaei, M. Knossow, Proc. Natl. Acad. Sci. 101 (2004) 10254–10259.
[18] T.J. Dolinsky, P. Czodrowski, H. Li, J.E. Nielsen, J.H. Jensen, G. Klebe, N.A. Baker, Nucleic Acids Res. 35 (2007) 522–525.
[19] B.R. Brooks, R.E. Bruccoleri, B.D. Olafson, D.J. States, S. Swaminathan, M. Karplus, J. Comput. Chem. 4 (1983) 187–217.
[20] J.P. Ryckaert, G. Ciccotti, Mol. Phys. 58 (1986) 1125–1136.
[21] J.P. Ryckaert, G. Ciccotti, H.J.C. Berendsen, J. Comput. Phys. 23 (1977) 327–341.
[22] M. Souaille, B. Roux, Comput. Phys. Commun. 135 (2001) 40–57.
[23] T.W. Allen, T. Bastung, S. Kuyucak, S.H. Chung, Biophys. J. 84 (2003) 2159–2168.